

# VESICLES ASSOCIATED WITH CALCIFICATION IN THE MATRIX OF EPIPHYSEAL CARTILAGE

H. CLARKE ANDERSON

From the Department of Pathology, State University of New York Downstate Medical Center,  
Brooklyn, New York 11203

## ABSTRACT

Vesicles have been identified within the cartilage matrix of the upper tibial epiphyseal plate of normal mice. They were seen at all levels within the plate and usually did not appear to be in contact with cartilage cells. Vesicles were concentrated within the matrix of the longitudinal septa from the proliferative zone downward. They varied considerably in size ( $\sim 300$  Å to  $\sim 1 \mu$ ) and in shape. They were bounded by unit membranes, and contained materials of varying density including, rarely, ribosomes. A close association was demonstrated between matrix vesicles and calcification: in the lower hypertrophic and calcifying zones of the epiphysis, vesicles were found in juxtaposition to needle-like structures removed by demineralization with ethylenediaminetetraacetate and identified by electron diffraction as hydroxyapatite and/or fluorapatite crystal structure—the former being indistinguishable from the latter for most cases in which electron diffraction methods are employed. Decalcification also revealed electron-opaque, partially membrane-bounded structures within previously calcified cartilage of the epiphyseal plate and underlying metaphysis which corresponded in size and distribution to matrix vesicles. It is suggested that matrix vesicles are derived from cells and that they may play a role in initiating calcification at the epiphysis.

## INTRODUCTION

Electron microscopic examination of the normal mouse epiphyseal plate has demonstrated vesicular structures within the cartilage matrix which may play a role in the process of calcification (1). These vesicles are similar to "cytoplasmic fragments" seen in induced cartilage undergoing hypertrophy and calcification (2). They are also comparable to amorphous osmophilic bodies present in calcifying cartilage of young guinea pigs and rats (3), and to "collections of vesicles and dense bodies" seen in articular cartilage (4). Within the epiphyseal plate, matrix vesicles show a characteristic pattern of distribution, described below, and are appropriately positioned to assume an integral role in calcification.

## MATERIALS AND METHODS

### *Tissue Preparation*

Upper tibial epiphyseal plates were obtained from weanling, ICR/Ha mice (Millerton Farms, Millerton, N.Y.) which were sacrificed by cervical dislocation. The plates were subdivided into approximately  $1 \times 3$  mm fragments. Fixation was carried out at  $4^{\circ}\text{C}$  in Veronal acetate-buffered osmium tetroxide (5) for 1 hr (five animals), or in cacodylate-buffered glutaraldehyde (6) for 1.5 hr (five animals). All glutaraldehyde-fixed tissue was postfixed in Veronal acetate-buffered osmium tetroxide for 1 hr. After fixation, tissues were dehydrated in graded alcohols and propylene oxide, embedded in Epon, and sectioned with glass and diamond knives on an LKB

microtome. Specimens were oriented in the Epon blocks so that sections would parallel the long axis of the tibia.

Thin sections were routinely stained for 5 min with lead citrate (7) preceded by 3% aqueous solution of uranyl acetate for 5 min. Some thin sections of decalcified material were stained with 10% aqueous solution of phosphotungstic acid for 30 min to demonstrate collagen fibrils. 1  $\mu$  thick sections were stained with toluidine blue solution (2) for light microscopy. An RCA EMU-3F electron microscope was used to examine and photograph thin sections.

### Decalcification

Epiphyses from four animals were fixed for 3 hr at 4°C in 0.1 M phosphate-buffered 4% aqueous solution of formaldehyde (USP), containing 5% ethylenediaminetetraacetate (EDTA) at pH 7.4. After fixation, tissues were given three ½-hr rinses in 0.1 M phosphate buffer, pH 8.3, containing 5% EDTA, and then three ½ hr incubations in similar buffer-EDTA solution at 37°C. This was followed by incubation in buffer-EDTA solution overnight at 37°C. Control tissues, fixed in formalin without EDTA, from five animals were processed through comparable rinses and incubations in 0.1 M phosphate buffer. Dehydration, embedding, and sectioning of decalcified tissues were carried out as described above.

### Electron Diffraction Methods

All electron diffraction analyses and interpretation of diffraction results were made at the General Telephone & Electronics Laboratories Inc., Bayside, N.Y. by Charles F. Tufts, assisted by T. A. Emma and Ruth Letendre.

The specimens used for analysis were prepared by the author in the form of sections from formalin-fixed, unstained tissues containing mineral deposits of varying density.

The modes of examination were transmission electron diffraction and selected area electron diffraction combined with selected area electron microscopy. For the transmission diffraction, an RCA-EMU-3F electron microscope was converted to a diffraction camera by replacing the intermediate lens of the microscope with the RCA-EMD-3 Diffraction Chamber MI-15356. The only lens employed was the double condenser system of the microscope. The distance from specimen to photographic plate (camera length) was 50 cm. Accelerating voltage was 100 kv. Electron beam diameter at the plate was 75  $\mu$ . Diffraction patterns were recorded on Kodak Projector Slide Plates (3 ¼ × 4 inches). The diffraction camera was calibrated by using a diffraction pattern composed of sharp rings obtained by photographing a dispersion of gold crystallites deposited by vacuum evaporation onto a carbon substrate. Most crystal-

lites ranged in size from 100 to 300 Å as determined by transmission electron diffraction-contrast microscopy.

The Philips EM 300 electron microscope with goniometer lens, rotation/tilt-type specimen holder and double condenser lens system was used for the selected area electron diffraction and selected area electron microscopy. Accelerating voltage was either 80 or 100 kv. The diameter of the field contributing to the selected area diffraction pattern (Fig. 13) and the selected area micrograph (Fig. 14) was approximately 2  $\mu$ . The selected area diffraction camera was calibrated by the same technique employed for the transmission mode. A carbon replica of a diffraction grating whose spacing was 2160 lines/millimeter was used to calibrate magnification for the selected area microscopy.

## RESULTS

### Distribution of Matrix Vesicles

The normal epiphyseal plate can be visualized as consisting of four general levels (Fig. 1). From top to bottom these include: (a) The reserve cell zone (8) consisting of a narrow band of rounded chondrocytes widely separated by matrix; (b) The proliferative zone, where cartilage cells appear flattened, are separated by narrow transverse matrix septa, and are arranged in longitudinal columns which are separated by longitudinal matrix septa; (c) The "hypertrophic" zone with columns of enlarged chondrocytes and lacunae; and (d) The calcifying zone which contains disintegrating chondrocytes and calcifying longitudinal septa.

Matrix vesicles (Figs. 2-7) were observed at all levels in the epiphyseal plate. Their uppermost occurrence appeared to be in the reserve cell zone near its junction with the overlying bony portion of the epiphysis. Localization of matrix vesicles within the longitudinal septa was apparent from the proliferative zone downward (Figs. 3, 5-7). Longitudinal septa were not identified in the reserve cell zone, but below this level they were easily recognizable because they contained collagen fibrils aligned parallel to the long axis of the tibia, whereas collagen fibrils in the transverse matrix septa and in a thin rim of perilacunar matrix were more randomly arranged (9). Matrix vesicles usually were not seen in the transverse septa from the proliferative zone downward. In the hypertrophic zone, concentration of vesicles in the longitudinal septa was evident.

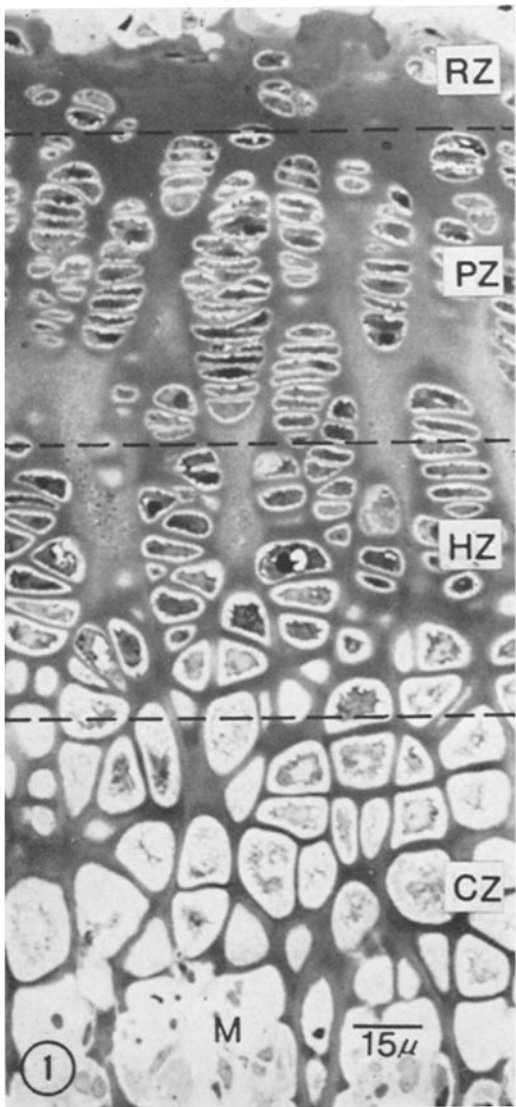


FIGURE 1 Levels of epiphyseal plate (top to bottom): *RZ*, reserve cell zone; *PZ*, proliferative zone; *HZ*, hypertrophic zone; *CZ*, zone of overt calcification and chondrocyte disintegration. A portion of the metaphysis (*M*) is present at the bottom.  $\times 600$ .

#### *Fine Structure of Matrix Vesicles*

Matrix vesicles were rounded, ovoid, or irregularly shaped (Figs. 2-7), and varied from  $\sim 300$  Å to  $\sim 1\mu$  in maximum dimension. At high magnification the outer membranes appeared to be composed of three layers (Figs. 4 and 10), thus conforming to the pattern of a unit membrane (10).

The contents of matrix vesicles showed considerable variation. Often the internal material was quite dense and apparently osmiophilic. Sometimes vacuolar structures and very rarely a few ribosomes were seen within vesicles. (Figs. 3 and 4).

Partially membrane-bounded, electron-opaque structures resembling matrix vesicles in size and distribution were observed within the calcified cartilage of the lower epiphyseal plate (Fig. 8) and in the subjacent metaphysis (Figs. 9 and 10) after calcium removal by EDTA.

Small, non-membrane-bounded, electron-opaque granules ( $\sim 250$  Å in maximum dimension) corresponding to the matrix granules previously described in ossifying cartilage of several species (2, 11-15) were seen scattered throughout the matrix of the mouse epiphysis (Figs. 3, 7, and 8). These were not noticeably concentrated within the longitudinal septa as were matrix vesicles, but were normally reduced in amount within the uppermost reserve cell zone (Fig. 2). Demineralization with EDTA did not appear to affect these small granules (Fig. 8) (16).

#### *Relation of Matrix Vesicles to Calcification*

Many vesicles were noted to be in contact with apatite-like material from the hypertrophic zone downward. Apparent calcium deposition was first recognized in the lower hypertrophic zone where single, elongated dense structures resembling hydroxyapatite were seen within and at the surfaces of matrix vesicles (Fig. 5). A similar picture was seen occasionally in the uppermost reserve cell zone near calcium deposits in the overlying bony portion of the epiphysis.

In the calcifying zone, vesicles were seen in association with clusters of similar needle-like structures (Figs. 6 and 7) identified as hydroxyapatite and/or fluorapatite by electron diffraction as described below. Early calcium deposition was usually found in the longitudinal septa. Transverse septa usually did not calcify (19, 17, 18).

In areas of heavy calcification, vesicles were obscured by apatite deposition. However, as indicated above, EDTA decalcification revealed partially membrane-bounded, vesicle-like structures within the matrix of calcified cartilage (Figs. 8-10).

In the decalcified metaphysis underlying the epiphyseal plate, spicules of previously calcified cartilage were invested with a layer of osteoid of varying thickness. Here scalloped boundaries were

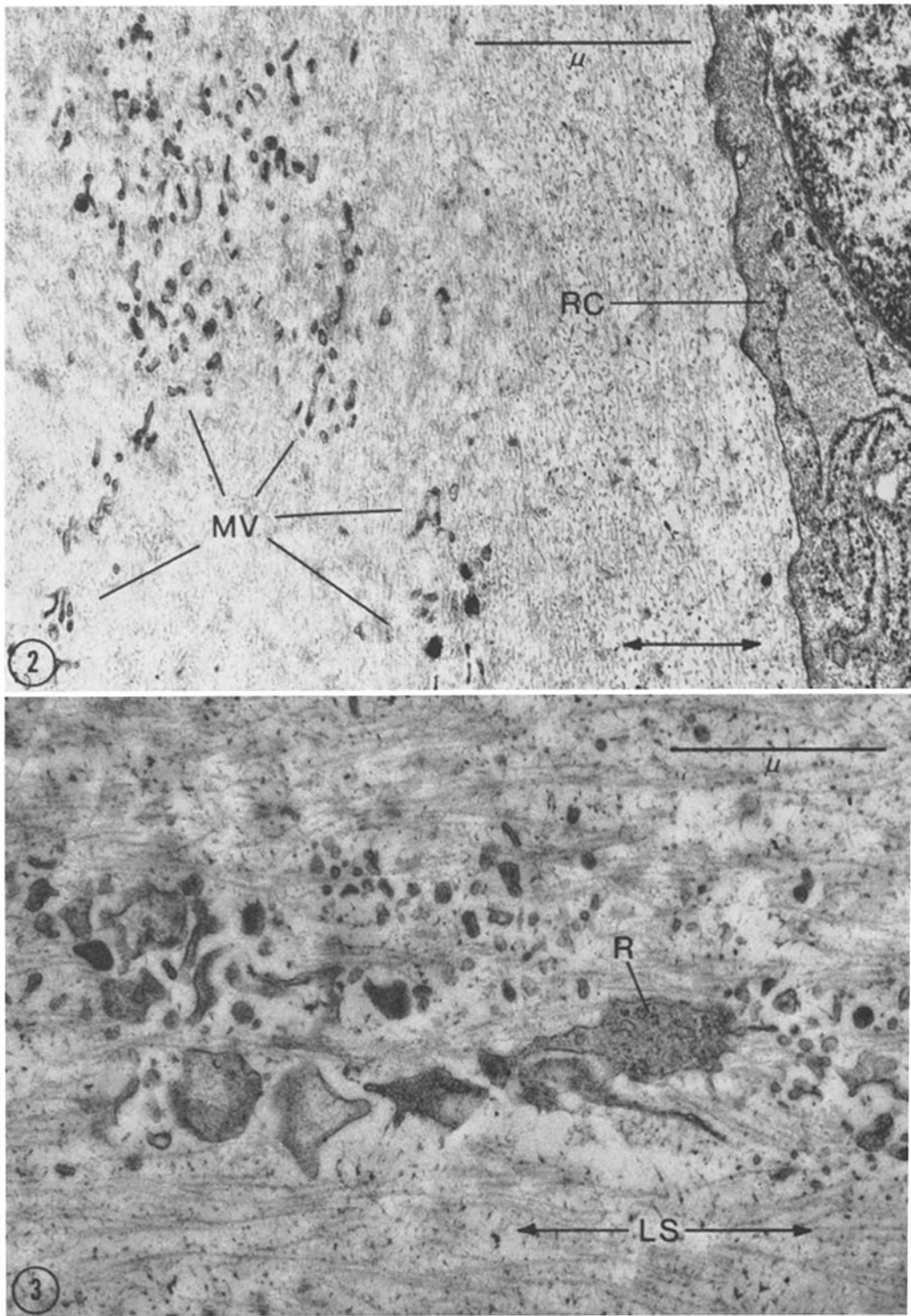


FIGURE 2 Matrix vesicles (MV) adjacent to a chondrocyte (RC) within the reserve cell zone. Longitudinal septa usually were not distinguishable at this level. The long axis of the tibia is indicated by arrows.  $\times 32,000$ .

FIGURE 3 Matrix vesicles within a longitudinal septum, upper hypertrophic zone, showing typical diversity of size, shape, and density. Ribosomes (R), (shown in greater detail in Fig. 4), are present within a vesicle. Collagen fibrils of the longitudinal septum (LS) parallel the long axis of the tibia which is indicated by arrows. Numerous tiny, electron-opaque particles, often referred to as matrix granules (12), are scattered throughout the matrix.  $\times 32,000$ .

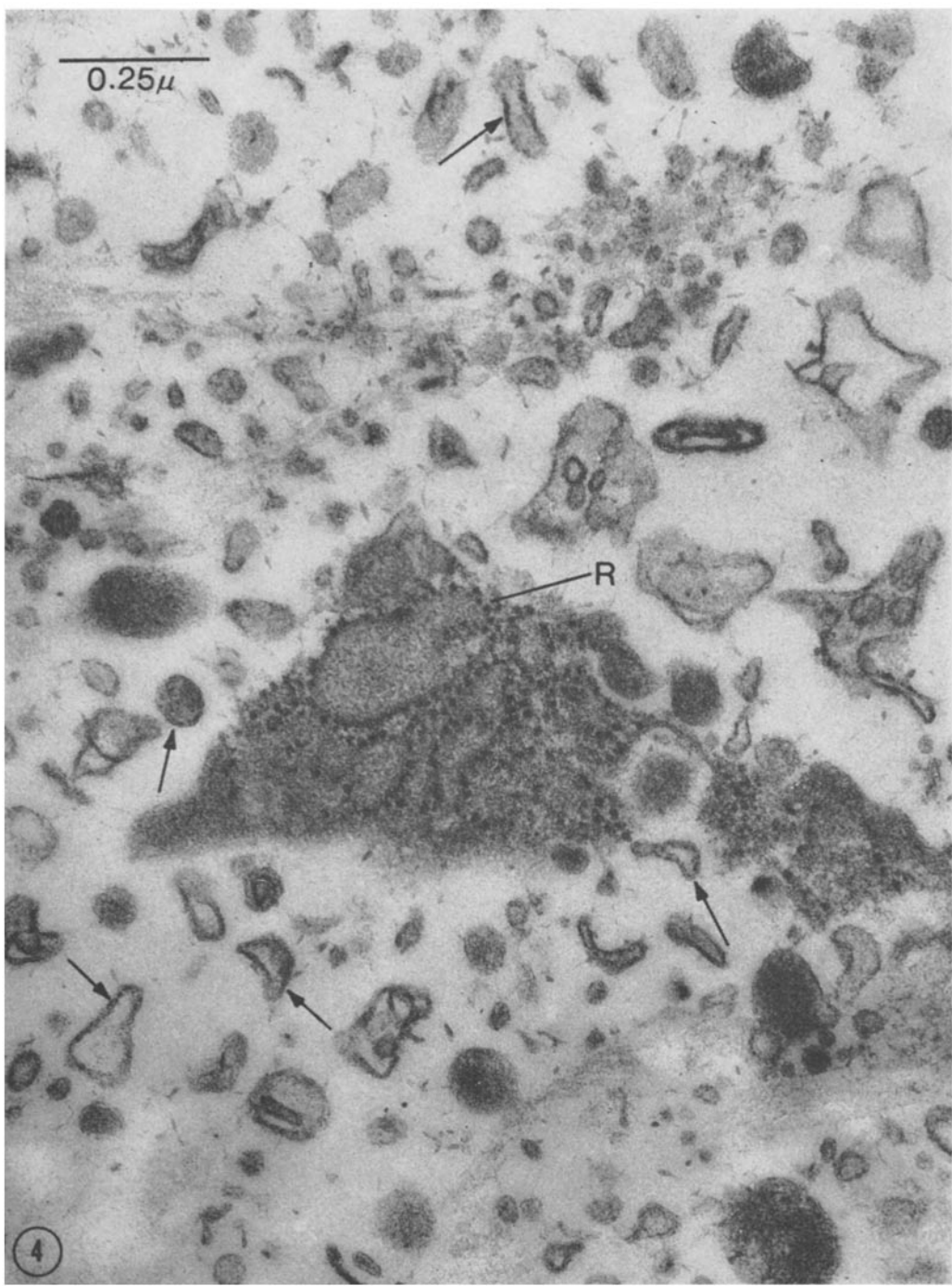


FIGURE 4 Matrix vesicles, upper hypertrophic zone. Ribosomes (*R*) are evident within a large cytoplasmic fragment. Several vesicles contain internal vacuole-like structures. Arrows indicate sectioned vesicles with typical three-layered unit membranes.  $\times 82,000$ .

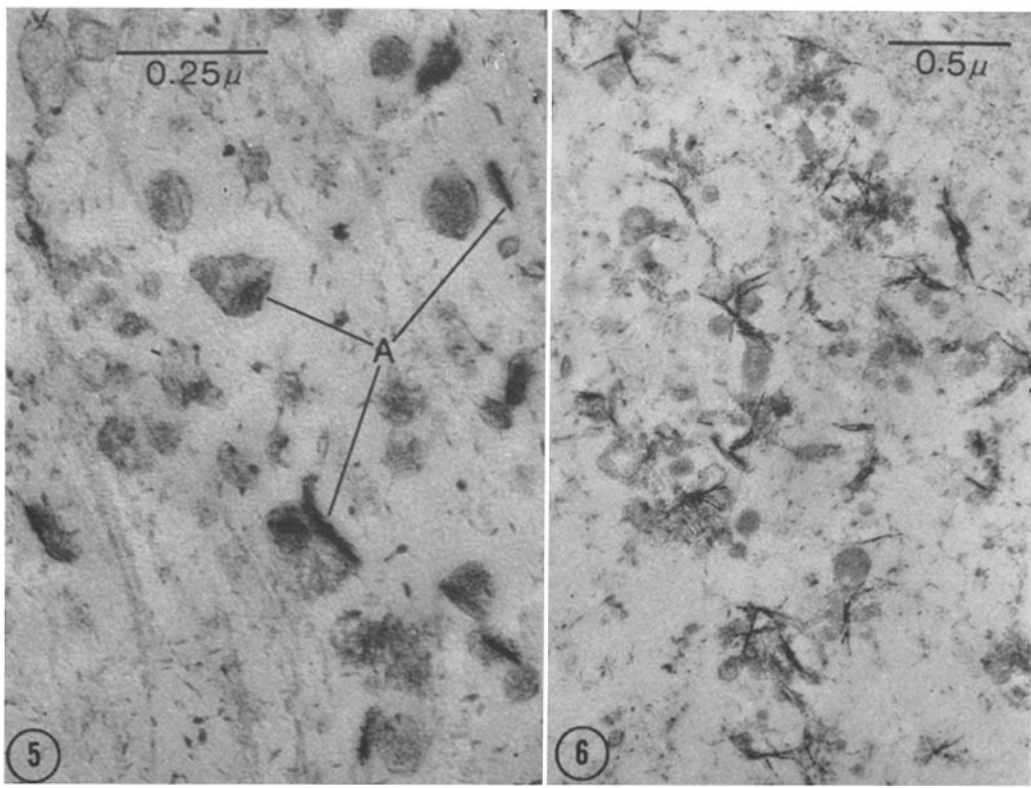


FIGURE 5 Lower hypertrophic zone. Matrix vesicles associated with electron-opaque, apatite-like shapes (*A*) measuring 60–120 Å in width and 400–1400 Å in length.  $\times 82,000$ .

FIGURE 6 Upper zone of calcification and chondrocyte disintegration. Associated matrix vesicles and apatite-like shapes.  $\times 32,000$ .

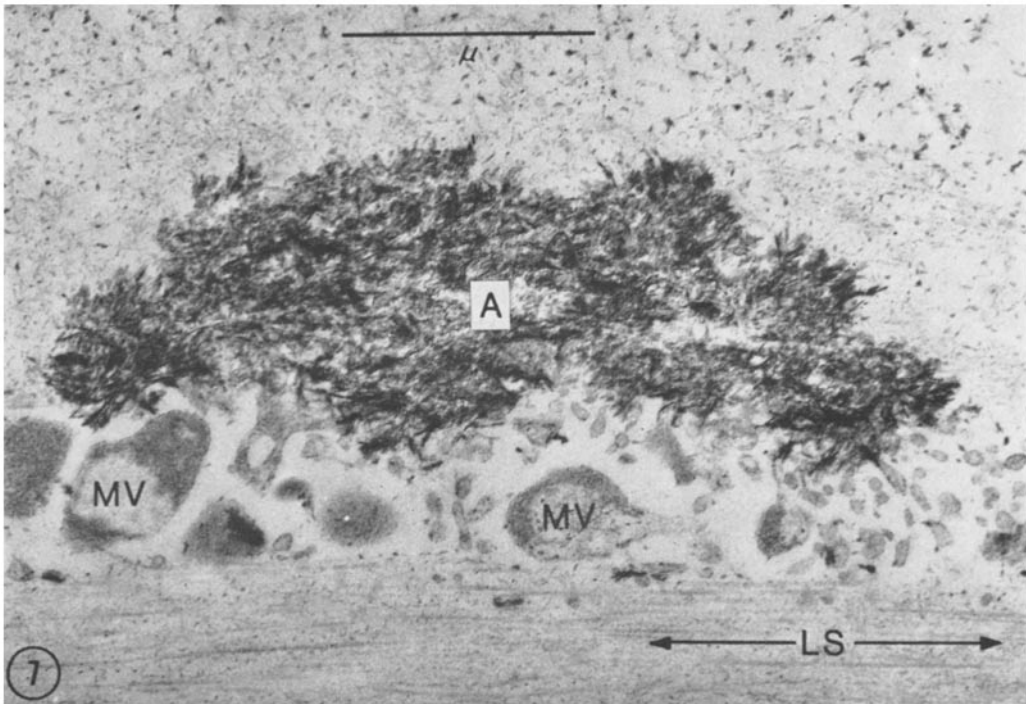


FIGURE 7 Midzone of calcification and chondrocyte disintegration. Fused globular masses of apatite-like material (*A*) are associated with matrix vesicles (*MV*) near the center of a longitudinal septum (*LS*). Tiny, dense matrix granules are evident in the matrix bordering a lacuna, upper right.  $\times 32,800$ .

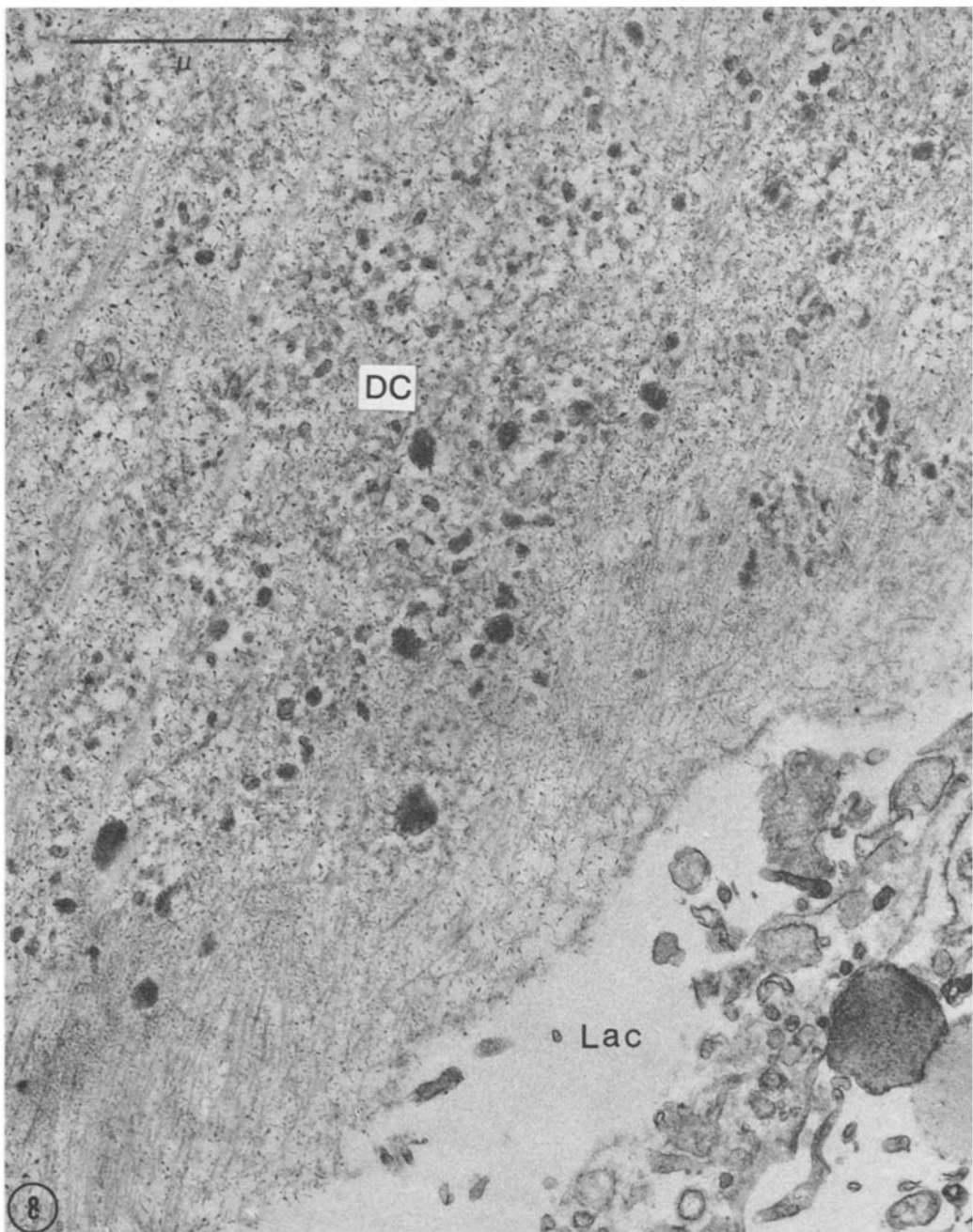
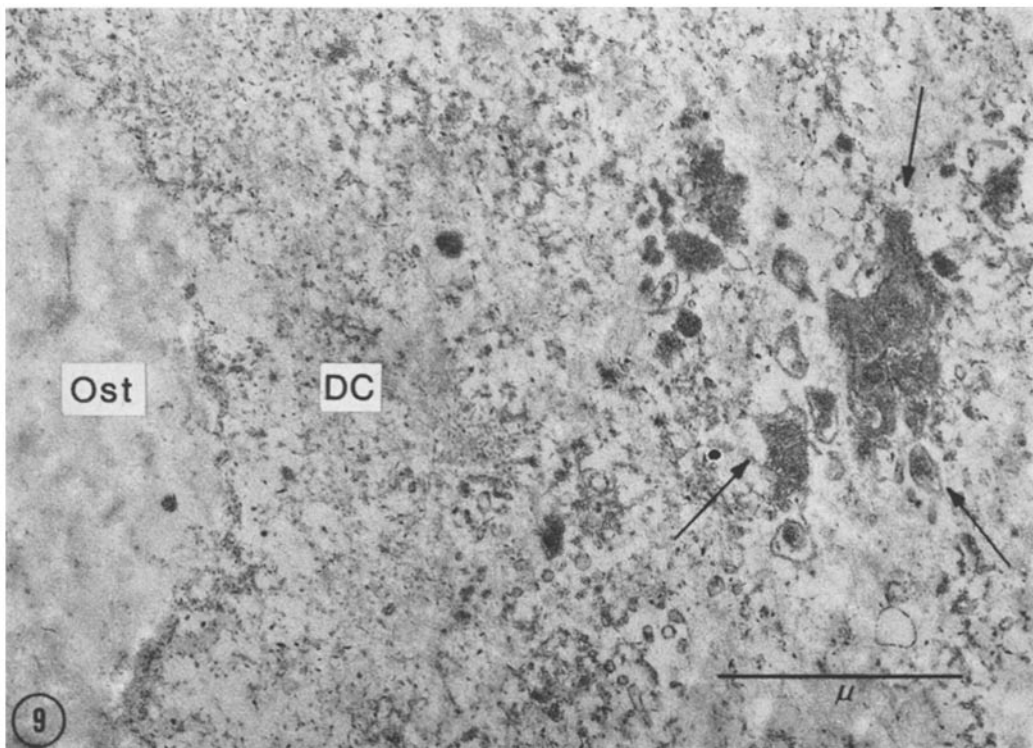


FIGURE 8 Lower calcified zone of epiphysis after EDTA demineralization. The decalcified cartilage matrix (*DC*) contains numerous, electron-opaque rounded structures corresponding in size and distribution to matrix vesicles. A lacuna (*Lac*) containing portions of a disintegrated chondrocyte is seen at lower right. Vesicle-free matrix separates chondrocyte fragments from apparent remnants of matrix vesicles. Numerous tiny particles seen throughout the cartilage matrix may represent matrix granules which were not removed by EDTA.  $\times 32,000$ .



**FIGURE 9** Metaphyseal area, after EDTA demineralization. Osteoid (*Ost*) is separated from decalcified cartilage (*DC*) by a scalloped border. Apparent remnants of matrix vesicles, indicated by arrows, and shown in greater detail in Fig. 10, are present in decalcified metaphyseal cartilage. Large collagen fibrils of osteoid were not well demonstrated after uranyl acetate and lead citrate staining shown here, but were easily recognized (Fig. 11) after PTA staining.  $\times 32,000$ .

recognized between cartilage matrix and osteoid (Fig. 9). Large, banded collagen fibrils of osteoid were easily distinguished from the small, indistinctly banded fibrils of cartilage after staining with phosphotungstic acid (Fig. 11).

#### *Electron Diffraction Data*

Table I summarizes the results of the electron diffraction analyses. Transmission diffraction and selected area diffraction obtained  $d(hkl)$  values that were very similar. Experimental results showed good agreement with  $d(hkl)$  values for hydroxyapatite and/or fluorapatite as reported in the American Society for Testing and Materials (ASTM) literature. Intensity values for the reflections obtained experimentally showed good agreement also with values reported in the literature.

Some preferred orientation of crystallites or texture of crystallites was observed by both modes

of examination as arcing of rings on the diffraction patterns (Figs. 12 and 13). The effect appeared stronger on patterns photographed by the selected area method (Fig. 13). Analysis of this arcing geometry showed that all crystallographic planes exhibited some degree of texture, except those with random orientation which contributed to the very strong and broad rings at 2.83-2.74 Å and 2.83-2.75 Å. These are reflections from (211), (112), and (300)  $hkl$  planes as shown in Table I. Randomness was observed also for some (222) planes.

The selected area micrograph (Fig. 14) shows a crystal population of medium concentration with lengths of the needle-like structures in the range of 600-1200 Å. A few Laue spots were present on the diffraction rings. These spots indicate the presence of a few crystallites larger than  $\sim 300$  Å; the continuous diffraction rings indicate the presence of many crystallites smaller than that size.

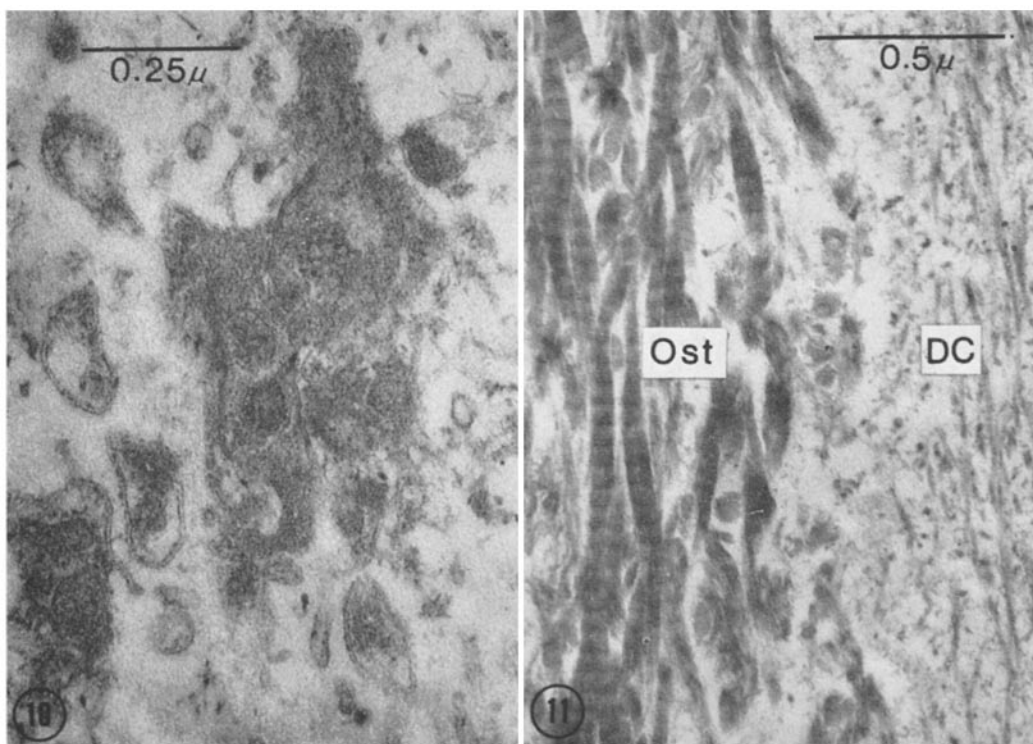


FIGURE 10 Apparent remnants of matrix vesicles, partially bounded by triple-layered membranes, are seen within decalcified cartilage of the metaphysis. (These structures are indicated by arrows in Fig. 9.)  $\times 82,000$ .

FIGURE 11 Junction of osteoid (*Ost*) and decalcified metaphyseal cartilage (*DC*) stained with PTA. The typical axial periodicity of collagen is seen in the large fibrils of osteoid; an axial period is not recognizable in the small fibrils of decalcified cartilage.  $\times 51,000$ .

## DISCUSSION

### *Origin of Matrix Vesicles*

The cellular origin of matrix vesicles is suggested by the presence of a surrounding unit membrane and the inclusion of vacuoles and rarely a few ribosomes. The mode of origin of matrix vesicles, and their pattern of movement within the epiphyseal plate, is as yet undetermined.

Bone growth is usually visualized as an upward movement of the epiphyseal plate relative to a fixed point in the mid-shaft (24). During this process matrix and cells are displaced downward relative to the receding reserve cell zone (25). The longitudinal matrix septa become calcified (9, 17, 18) and then persist in the metaphysis where they serve as a scaffolding for the deposition of new bone (25). On the other hand, cartilage cells and trans-

verse septa are resorbed and disappear during the process of metaphyseal capillary invasion (9).

It is possible that vesicles arise from budding or disintegrating cells in the upper portion of the epiphyseal plate, and then become entrapped in matrix which eventually will serve as longitudinal septa. Vesicles could then move with this matrix as it becomes first calcified and then incorporated into the metaphysis.

An alternative possibility is that matrix vesicles are formed and dispersed from disintegrating chondrocytes in the zone of calcification. This possibility appears less likely since it would require movement of vesicles upward into the reserve cell zone against a downward flow of cells and matrix. Also if disintegrating chondrocytes in the calcifying zone were contributing vesicles, one would expect a heavier concentration of vesicles to exist

TABLE I  
*Experimental Electron Diffraction Data Obtained from a Section of Formalin-Fixed Mouse Epiphysis Compared  
 with X-ray Diffraction Data for Hydroxyapatite and Fluorapatite as Reported in the Literature*

Experimental Data				Data From Literature (ASTM)					
Transmission diffraction		Selected area diffraction		Hydroxyapatite 9-432			Fluorapatite 15-876		
d(hkl) Å	I	d(hkl) Å	I	d(hkl) Å	P I/I <sub>1</sub>	hkl	d(hkl) Å	D I/I <sub>1</sub>	hkl
3.74*				VVW					
3.41	M-S	3.40	S	3.44	40	002	3.442	40	002
		3.18-	VW	3.17	12	102	3.167	14	102
		3.09	B	3.08	18	210	3.067	18	210
2.83- 2.75	S B	2.83-	VS	2.814	100	211	2.800	100	211
		2.74	B	2.778	60	112	2.772	55	112
				2.720	60	300	2.702	60	300
2.30- 2.25	VW D	2.25	VW	2.296	8	212	2.289	8	212
				2.262	20	310	2.250	20	310
				2.228	2	221	2.218	4	221
1.94	W	1.93	VW	1.943	30	222	1.937	25	222
				1.871	6	320	1.862	4	320
				1.841	40	213	1.837	30	213
1.84	W	1.83	VW	1.806	20	321	1.797	16	321
				1.754	16	402, 303	1.748	14	402
				1.722	20	004, 411	1.722	16	004
1.70	W-M	1.71	W	1.684	4	104	1.684	<1	104
1.47- 1.44	VW B			1.503	10	214, 421	1.501	4	214
				1.474	12	502	1.497	4	421
				1.465	4	510	1.468	8	502
1.10‡	W			(Plus additional lines not listed on file card.)			(Plus 45 lines to 0.99 Å not listed on file card.)		

*Explanation of Symbols*

Transmission diffraction: Data obtained with the RCA-EMU-3F electron microscope converted to a 50 cm diffraction camera.

Selected area diffraction: Data obtained with the Philips EM 300 electron microscope set for selected area mode.

Hydroxyapatite (9-432): Calcium Hydroxide Orthophosphate;  $\text{Ca}_5(\text{PO}_4)_3(\text{OH})$ ; hexagonal with S.G. =  $\text{P}6_3/m$ ; x-ray powder diffraction literature of ASTM, file card reference 9-432 (19).

Fluorapatite (15-876): Calcium Fluoride Phosphate;  $\text{Ca}_5\text{F}(\text{PO}_4)_3$ ; hexagonal with S.G. =  $\text{C}2\text{h}-\text{P}6/m$  x-ray powder diffraction literature of ASTM, file card reference 15-876 (20).

d(hkl) Å: Interplanar spacings of the crystal lattice expressed in Angstrom Units (Å) (21).

I: Relative intensities of rings on diffraction patterns obtained by visual inspection for the experimental work (VS, very strong, S, strong, M, medium, M—S, medium to strong, W, weak, W-M, weak to medium, VW, very weak, VVW, very, very weak, B, broad, D, diffuse.)

P—I/I<sub>1</sub>: Relative intensities obtained by photometer.

D—I/I<sub>1</sub>: Relative intensities obtained by diffractometer.

hkl: Miller indices (22).

\* Unidentified reflection.

‡ ASTM data does not include this reflection. Frank et al. (23) reported an observed d(hkl) of 1.10 Å and a calculated value of 1.095 Å for the 702 and 532 Miller indices.

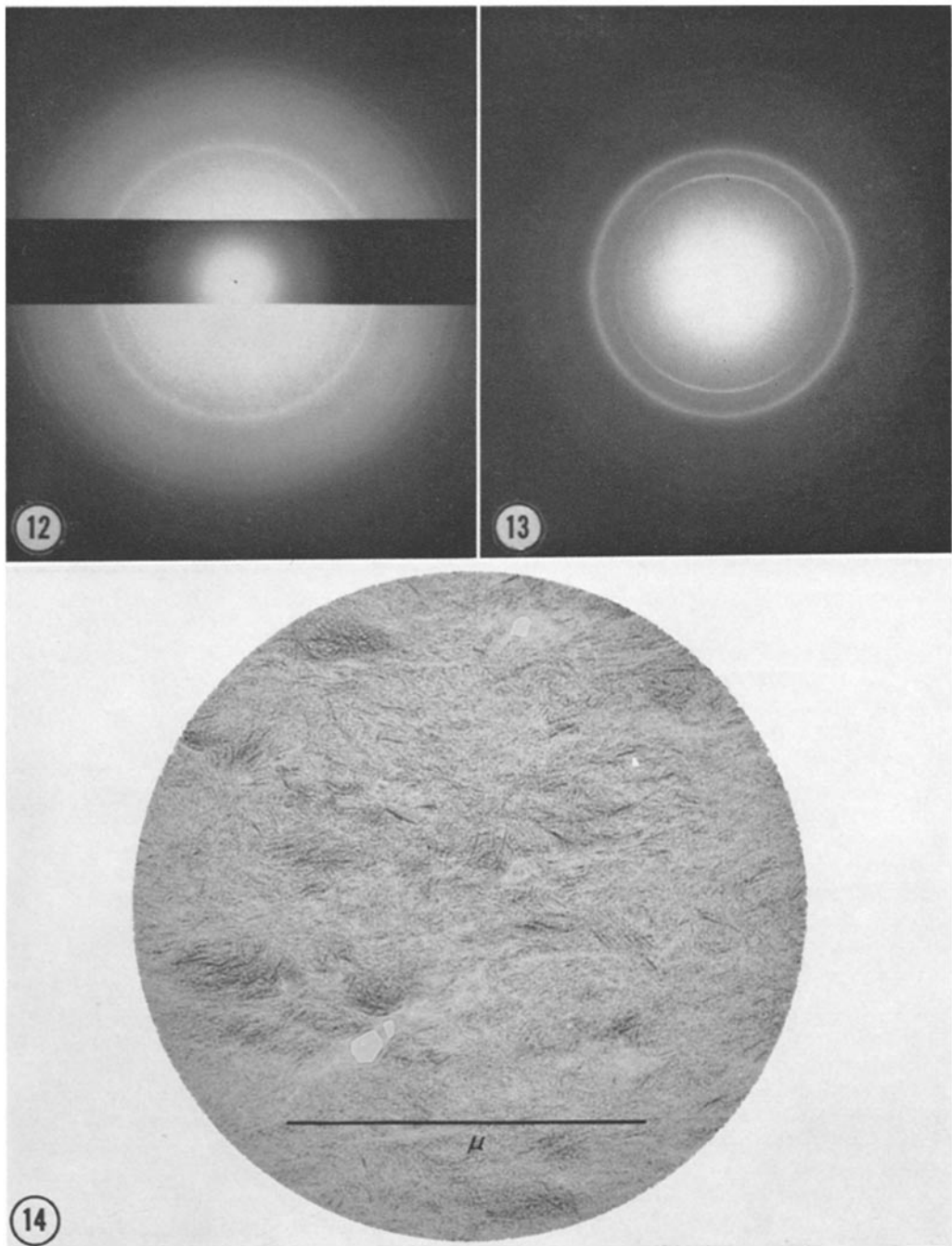


FIGURE 12 Transmission electron diffraction pattern obtained from a section of formalin-fixed, unstained mouse epiphysis by the use of 100-kv electrons and 50-cm diffraction camera length.

FIGURE 13 Selected area electron diffraction pattern obtained from a section of formalin-fixed, unstained mouse epiphysis by the use of 80-kv electrons. Arcing of some diffraction rings indicates that some crystals exhibit preferred orientation.

FIGURE 14 Selected area electron micrograph showing exact field sampled by the electron beam to produce the electron diffraction pattern of Fig. 13. Accelerating voltage was 80 kv.  $\times 51,000$ .

in the matrix immediately surrounding these cells, but, in fact, there is usually a layer of matrix investing the degenerating cells which contains very few vesicles (Fig. 8).

The cell(s) of origin of matrix vesicles remains undetermined. Chondrocytes in the upper epiphyseal plate would seem to be a likely source, although origin from chondrocytes at lower levels or from cells outside of the epiphyseal plate is possible.

#### *Interpretation of Electron Diffraction Data*

The broad reflection extending from 2.83–2.75 Å observed by transmission diffraction and from 2.83 to 2.74 Å observed by selected area diffraction is interpreted as line-broadening producing an integration of the three strongest reflections of hydroxyapatite and/or fluorapatite (Table I). In the case of electron diffraction data reported by Frank et al. (23), only the 2.74 Å  $d(hkl)$  value was reported.

In the electron diffraction method, line-broadening can be caused by chemical heterogeneity, small crystal size in the range below 100 Å, strain effects within the crystal lattice, and/or lack of instrumental resolution. In studies made previously at the General Telephone & Electronics laboratories to relate line-broadening effects with crystal size, for the instruments employed in this work, dispersions of gold crystals with crystal sizes ranging from 10 to 1000 Å established that sizes below 100 Å produced line-broadening effects, sizes from 100 to 300 Å produced sharp ring patterns, and sizes from 300 to 1000 Å produced discrete Laue spots that tended to form rings. Where rings were sharp, accuracy of analysis was better than  $\pm 0.1\%$  for transmission diffraction and better than  $\pm 0.3\%$  for the selected area method, with assumed correct values being the x-ray powder diffraction data reported in the ASTM literature for gold structure. From this it is concluded that line-broadening observed during the experimental work was not caused by lack of instrumental resolution. This leaves small crystallite size, chemical heterogeneity, and/or strain within the crystals as probable causes of line-broadening.

#### *Nature of Matrix Vesicles*

Matrix vesicles were discrete and did not appear to be cytoplasmic projections from cartilage cells. Repeated examination following various types of fixation did not show significant connec-

tions between cartilage cells and vesicles, and usually there was a vesicle-free zone separating the former from the latter.

It is possible that some or all of these vesicles represented lysosomes. The morphology of many vesicles resembled that of lysosomes, and the release of lysosomes from cells is possible, since leukocytes are believed to release their lysosomal granules during inflammation (26). Further studies of the vesicles to determine their enzymatic properties will be necessary to support or reject this possibility.

The only structural feature common to most matrix vesicles was the outer membrane. Vesicular contents varied tremendously in amount, density, and composition (Fig. 4). Some vesicles were extremely dense and apparently osmiophilic, suggesting the presence of lipid (2). Also, it is likely that lipid was present in the investing membranes. This is interesting in connection with the description by Irving of sudanophilic material in calcifying epiphyseal cartilage (27). Matrix vesicles may represent the fine structural counterpart of this material. They also may be comparable to the amorphous material which was seen in association with early calcium deposition at the epiphysis by Robinson and Cameron (14). The apparent remnants of matrix vesicles described above within decalcified cartilage (Fig. 8) may correspond to the dense centers seen by the author (2) within clusters of apatite crystals in induced cartilage, and may be comparable to the amorphous material identified by Takuma (15) in the decalcified epiphyseal plate.

As stated above, matrix vesicles probably are comparable to the "amorphous, roundish bodies" shown by Bonucci (3) to be associated with calcification of costal and epiphyseal cartilage. Nevertheless, Bonucci's amorphous bodies appear to differ from matrix vesicles in a number of important ways: outer membranes were not described around amorphous bodies, which were said to be homogeneous and lacking in cytoplasmic organelles; amorphous bodies were not described within the reserve cell zone, and they were not identified in calcified cartilage after EDTA de-mineralization.

Recognition of these bodies as vesicles possessing organelles such as membranes, vacuoles, and, rarely, ribosomes leads to an entirely different concept of their origin and possible function in calcification. Bonucci, proceeding on the assumption

tion that the bodies were truly amorphous, has suggested that they may form within the matrix as the result of cellular enzymatic activity and may be related to "elastoid," which has been visualized (28) as a mixture of calcium complexes, fibrous proteins, mucoproteins, lipoproteins, and other substances. The idea that amorphous bodies form by chemical reaction within the matrix is in sharp contrast to the idea that vesicles form as membrane-bounded subcellular particles which could retain enzymatic and other cellular functions. The presence of a membrane suggests the possibility of ionic concentration gradients across the membrane, and even the possibility of active calcium-binding.

#### *Matrix Vesicles and Calcification*

The intimate association of matrix vesicles with apatite deposition in the longitudinal septum was clear cut (Figs. 5-7). Initial deposition of apatite-like material in juxtaposition to matrix vesicles (Figs. 5-7) suggests that the latter may, in some way, promote apatite nucleation. Assuming this to be the case, two general mechanisms of vesicle function suggest themselves.

One possibility is that matrix vesicles behave as lysosomes. Lysosomal activity has been demonstrated in cartilage of developing embryonic limb buds (29), and lysosomal enzymes have been im-

plicated in the calcification mechanism (30). Release of hydrolytic enzymes from vesicles could cause an alteration in the physical state of the surrounding matrix (31), possibly accompanied by a local reduction in protein-polysaccharide (31, 32). This change could render collagen (33) or other matrix factors more calcifiable.

A second possibility is that matrix vesicles may bind calcium (1) as do the calcium-binding vesicles of peripheral nerve (34) and cardiac (35) and skeletal muscle (36, 37). In this hypothesis, calcium-binding would lead to a localized accumulation of calcium and a resulting precipitation of hydroxyapatite in the vicinity of vesicles. The fact that early deposition of apatite-like material was seen often within vesicles (1, 3) would appear to support the idea of calcium-binding.

Clearly, more work will have to be done to define the function of matrix vesicles.

This work was supported by United States Public Health Service grants No. CA-10052 and CA-06081.

The author wishes to express his gratitude to Miss Priscilla Coulter for her expert technical assistance.

The work in electron diffraction was contributed by the General Telephone & Electronics Laboratories Inc., Bayside, N.Y.

*Received for publication 30 April 1968, and in revised form 18 November 1968.*

#### REFERENCES

1. ANDERSON, H. C. 1968. Vesicles in the matrix of epiphyseal cartilage: fine structure, distribution and association with calcification. *In Proceedings of the 4th European Regional Conference on Electron Microscopy.* D. S. Bocciarelli, editor. Tipografia Poliglotta Vaticana, Roma. 437.
2. ANDERSON, H. C. 1967. Electron microscopic studies of induced cartilage development and calcification. *J. Cell Biol.* 35:81.
3. BONUCCI, E. 1967. Fine structure of early cartilage calcification. *J. Ultrastruct. Res.* 20:33.
4. PALFRY, A. J., and D. V. DAVIES. 1966. The fine structure of chondrocytes. *J. Anat.* 100:213.
5. PALADE, G. E. 1952. A study of fixation for electron microscopy. *J. Expt. Med.* 95:285.
6. SABATINI, D. D., K. BENSCHE, and R. J. BARRNETT. 1963. Cytochemistry and electron microscopy. The preservation of cellular ultrastructure and enzymatic activity by aldehyde fixation. *J. Cell Biol.* 17:19.
7. REYNOLDS, E. S. 1963. The use of lead citrate at high pH as an electron-opaque stain in electron microscopy. *J. Cell Biol.* 17:208.
8. KEMBER, N. F. 1960. Cell division in endochondral ossification. A study of cell proliferation in rat bones by the method of tritiated thymidine autoradiography. *J. Bone Joint Surg. B. Brit.* Vol. 42:824.
9. SCHENK, R. K., D. SPIRO, and J. WIENER. 1967. Cartilage resorption in the tibial epiphyseal plate of growing rats. *J. Cell Biol.* 34:275.
10. ROBERTSON, J. D. 1959. The ultrastructure of cell membranes and their derivatives. *Biochem. Soc. Symp.* 16:3.
11. GODMAN, G. C., and K. R. PORTER. 1960. Chondrogenesis studied with the electron microscope. *J. Biophys. Biochem. Cytol.* 8:719.
12. MATUKAS, V. J., B. J. PANNER, and J. L. ORBISON. 1967. Studies on ultrastructural identification and distribution of protein-polysaccharide in cartilage matrix. *J. Cell Biol.* 32:365.
13. REVEL, J. P., and E. D. HAY. 1963. An auto-

- radiographic and electron microscopic study of collagen synthesis in differentiating cartilage. *Z. Zellforsch. Mikroskop. Anat.* **61**:110.
14. ROBINSON, R. A., and D. A. CAMERON. 1956. Electron microscopy of cartilage and bone matrix at the distal epiphyseal line of the femur in the newborn infant. *J. Biophys. Biochem. Cytol.* **2** (Suppl.):253.
  15. TAKUMA, S. 1960. Electron microscopy of the developing cartilaginous epiphysis. *Arch. Oral Biol.* **2**:111.
  16. ANDERSON, H. C., and P. R. COULTER. 1968. Effects of EDTA hyaluronidase and collagenase on epiphyseal cartilage matrix. In Proceedings of the 26th Annual Meeting of the Electron Microscopy Society of America. C. J. Arceneaux, editor. Claitors Publishing Division, Baton Rouge. 56.
  17. DODDS, G. S. 1932. Osteoclasts and cartilage removal in endochondral ossification of certain mammals. *Amer. J. Anat.* **50**:97.
  18. KNESE, K. H., and A. M. KOOP. 1961. Elektronenmikroskopische beobachtungen über die zellen in der eröffnungzone des epiphysenknorpels. *Z. Zellforsch. Mikroskop. Anat.* **54**:1.
  19. ASTM Inorganic Index to the Powder Diffraction File. 1967. Powder Diffraction Index Set 17i. American Society for Testing and Materials. Philadelphia, Pa. 443.
  20. ASTM Inorganic Index to the Powder Diffraction File. 1967. Powder Diffraction Index Set 17i. American Society for Testing and Materials. Philadelphia, Pa. 442.
  21. BARRETT, C. S. 1952. The Structure of Metals. McGraw-Hill Book Company, New York. 2nd edition. 75.
  22. BARRETT, C. S. 1952. The Structure of Metals. McGraw-Hill Book Company, New York. 2nd edition. 8.
  23. FRANK, R. M., R. F. SOGNNAES, and R. KERN. 1960. Calcification of dental tissues with special reference to enamel ultrastructure. In Calcification in Biological Systems, R. F. Sognnaes, editor. American Assn. for the Advancement of Science, Washington, D.C. 163.
  24. LEBLONDE, C. P., and R. C. GREULICH. 1956. Autoradiographic studies of bone formation and growth. In The Biochemistry and Physiology of Bone. G. H. Bourne, editor. Academic Press Inc. New York. 325.
  25. SISSONS, H. A. 1956. The growth of bone. In The Biochemistry and Physiology of Bone. G. H. Bourne, editor. Academic Press Inc., New York. 443.
  26. HIRSCH, J. G., and Z. A. COHN. 1963. Leucocyte lysosomes. In Cell-Bound Antibodies. B. Amos and H. Koprowski, editors. Wistar Institute Press, Philadelphia. 45.
  27. IRVING, J. T. 1963. The sudanophil material at sites of calcification. *Arch. Oral Biol.* **8**:735.
  28. URIST, M. R. 1964. Recent advances in the physiology of calcification. *J. Bone Joint Surg. A. Amer. Vol.* **46**:889.
  29. LUCY, J. A., J. T. DINGLE, and H. B. FELL. 1961. Studies on the mode of action of excess vitamin A. 2. The possible role of intracellular proteases in the degradation of cartilage matrix. *Biochem. J.* **79**:500.
  30. JIBRIL, A. D. 1967. Phosphates and phosphatases preosseous cartilage. *Biochim. Biophys. Acta.* **141**:605.
  31. MATUKAS, V. J., and G. A. KRIKOS. 1968. Evidence for changes in protein-polysaccharide associated with the onset of calcification in cartilage. *J. Cell Biol.* **39**:43.
  32. HIRSCHMAN, A., and D. D. DZIEWAITSKI. 1966. Protein-polysaccharide loss during endochondral ossification. Immunochemical evidence. *Science* **154**:393.
  33. GLIMCHER, M. J. 1961. The role of the macromolecular aggregation state and reactivity of collagen in calcification. In Macromolecular Complexes. M. V. Edds, Jr., editor. The Ronald Press Co., New York. 53.
  34. LIEBERMAN, E. M., R. F. PALMER, and G. H. COLLINS. 1967. Calcium ion uptake by Crustacean peripheral nerve subcellular particles. *Exp. Cell Res.* **46**:412.
  35. CARSTEN, M. E. 1964. The cardiac calcium pump. *Proc. Nat. Acad. Sci. U.S.A.* **52**:1456.
  36. EBASHI, S., and F. LIPMANN. 1962. Adenosine triphosphate-linked concentration of calcium ions in a particulate fraction of rabbit muscle. *J. Cell Biol.* **14**:389.
  37. HASSELBACH, W., and M. MAKINOSE. 1960. Die calciumpumpe der "Erschlaffungsgrana" des muskels und ihre abhangigkeit von der ATP-spaltung. *Biochem. Z.* **333**:518.